Impact of flexible succinate connectors on the formation of tetrasulfonylcalix[4]arene based nano-sized polynuclear cages: structural diversity and induced chirality study

Mariia V Kniazeva, Alexander S Ovsyannikov, Aida I Samigullina, Daut R Islamov, Aidar T Gubaidullin, Pavel V Dorovatovskii, Vladimir A Lazarenko, Svetlana E Solovieva, Igor S Antipin, Sylvie Ferlay

Impact of flexible succinate connectors on the formation of tetrasulfonylcalix[4]arene based Nano-sized polynuclear cages: structural diversity and induced chirality study

Mariia V. Kniazeva,[a] Alexander S. Ovsyannikov,[a]* Aida I. Samigullina,[a] Daut R. Islamov,[b] Aidar T. Gubaidullin,[a] Pavel V. Dorovatovskii,[d] Vladimir A. Lazarenko,[d] Svetlana E. Solovieva,[c] Igor S. Antipin,[c] Sylvie Ferlay[e]*

The building of new Supramolecular Coordination Containers obtained through the linking of tetrasulfonylcalix[4]arene (**3**-4H) based transition metal tetra- or trinuclear clusters by succinic acid (**suc**) as a flexible aliphatic connector possessing high conformational mobility and rotational freedom, produced a variety of three different polynuclear species in the crystalline phase, which were characterized by X-ray diffraction on single crystals and powder. In the case of Co^{II} and Ni^{II} cations, the formation of unique chiral-induced isomorphous supramolecular architectures generated by interconnection of dimeric M_8-cages with the co-crystallized $M(OH)_2DMF_4$ neutral species *via* H-bonding was observed. Moreover, it was found that, in contrast to what was observed with Ni^{II} cations, the use of Cobalt(II) ions in the same multicomponent system, led to the formation of achiral M_8-cages which was characterized by the presence of both left- and right-handed succinic acid moieties within the supramolecular entity structure. Finally, the coordination of Zn^{II} cations with **3**-4H and succinic acid produced the generation of dimeric M_6-cages where two trinuclear $[Zn_3\text{-}\mathbf{3}]^{2+}$ cationic clusters were bound by two succinic carboxylate units.

Introduction

Nanosized discrete supramolecular entities such as metal-organic coordination cages[1,2,3] or polyhedra[4] are the object of particular attention, due to their wide potential applications in biological, medical, environmental, and industrial fields.[5,6,7,8] The key strategy for designing such Supramolecular Coordination Cages (SCCs) with desired properties is based on the rational choice of the used components. The controlled formation, in self-assembly conditions, of coordination compounds tunable different shape and size may be achieved within the ligand scaffold, by pointing the coordinating sites in preorganized fashion, for example. In this respect, the use of macrocyclic compounds of the metacyclophane family[9,10] is a powerful tool to grow large coordination capsules, due to their unlimited possibilities of functionalization of the metacyclophane moiety.

Among the accessible metacyclophanes, one should mention the calix[4]arene[11] (**1**-4H, figure 1) and, especially, thiacalix[4]arene[12] (**2**-4H, figure 1) as well as tetrasulfonylcalix[4]arene[13,14] (**3**-4H, figure 1) based polydentate macrocyclic ligands, owing to the preorganized orientation of the coordinating sites, when adopting their *cone* conformation. They possess the fascinating ability to form various polynuclear homo- and heterometallic clusters when coordinated to d/f metal cations[15,16,17,18,19] exhibiting attractive luminescence properties[20,21,22,23,24,25,26] and magnetic behavior.[27,28,29,30,31,32,33,34] Also using **1**-4H and **2**-4H in *cone* conformation as a building species, the formation of extended coordination networks in the crystalline phase was extensively documented.[35]

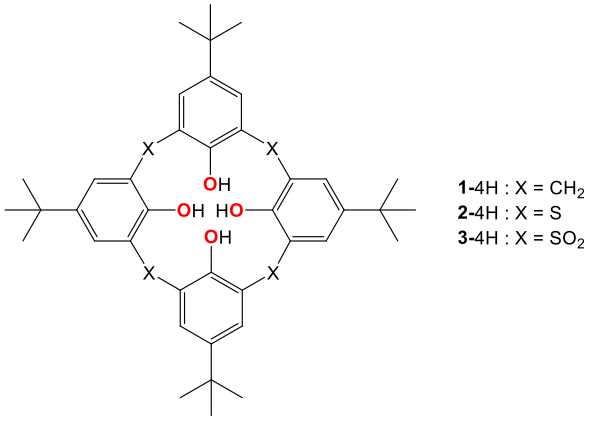

Figure 1. Classical p-*tert*-butylcalix[4]arene (**1**-4H), p-*tert*-butylthiacalix[4]arene (**2**-4H) and p-*tert*-butyl-tetrasulfonylcalix[4]arene (**3**-4H).

For the formation of clusters, the coordination of calixarene to metallic cations leads to nanozised species where the cluster core is maintained between the oppositely disposed ligands. Through this approach, the use of unsubstituted $\mathbf{1}^{4-}$, behaving as a tetradentate coordination ligand containing four O-donor atoms, leads to a mononuclear species when combined with d metallic cations, whereas in the case of multidentate $\mathbf{3}^{4-}$ or $\mathbf{2}^{4-}$ ligand, the formation of tetranuclear species is generally observed (figure 2).

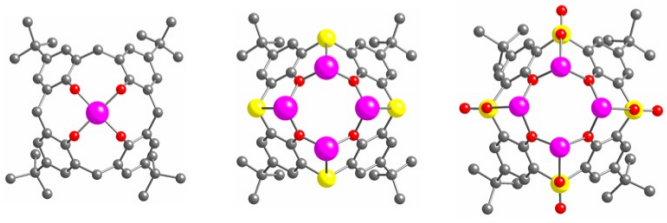

Figure 2. Differences in coordination mode of *p-tert*-butylcalix[4]arene ($\mathbf{1}^{4-}$), *p-tert*-butylthiacalix[4]arene ($\mathbf{2}^{4-}$) and *p-tert*-tetrasulfonylcalix[4]arene ($\mathbf{3}^{4-}$) towards metallic d cations (purple spheres).

Moreover, it was shown that *3d* metal based clusters supported by thiacalix[4]arene **2**-4H or tetrasulfonylcalix[4]arene **3**-4H platforms can be linked by the polydentate N-[36,37] and/or- O-donor co-ligands (linkers) leading to the formation of polynuclear compounds of various nuclearities and presenting hierarchical pores, which are able to exhibit different smart properties such as selective adsorption, catalysis, encapsulation, sensing or separation.[38,39,40]

The three components approach involving tetrasulfonylcalix[4]arene **3**-4H, metallic cations and polytopic carboxylate ligands has been successfully studied for the formation of polyhedral cages, involving the $[\mathbf{3}\text{-}M_4(OH_2)]^{4+}$ units ("shuttlecock"-like building blocks, figure 3).[41] Depending on the nature of the used ligand L, different types of SCCs presenting various nuclearities may be obtained (see figure 3): dimeric M_8[42], square-like M_{16}[43,44], and octahedral M_{24},[45],[44,45,46,47,48,49,50,51,52,53] (M = Co, Ni or Zn) nanosized cages presenting appealing catalytic properties and also drug delivery abilities, have been reported during the last decade.

To the best of our knowledge, only linkers possessing rigid V-shaped and linear geometry lead to high nuclearity clusters (M_{16} or M_{24} cages), as shown in figure 3. In addition and as already mentioned, smaller containers have been reported, M_8 coordination compounds (M = Co^{II}, Ni^{II} and sometimes Zn^{II}), while using dicarboxylate connectors like angular flexible dicarboxylate linkers with phenyl groups[54,55,56] camphoric acid,[57] pyridinium-dicarboxylate[58,59] 1,2-benzenedicarboxylic acid or 2,3-naphthalenedicarboxylic acid.[60] One can see that the used connectors are either short or present a point a flexibility between the phenyl groups spacers. The formed M_8 SCCs present two types of cavities: two *exo* and one *endo* where the $[\mathbf{3}\text{-}M_4(OH_2)]^{4+}$ have been fused by the L connectors (figure 3).

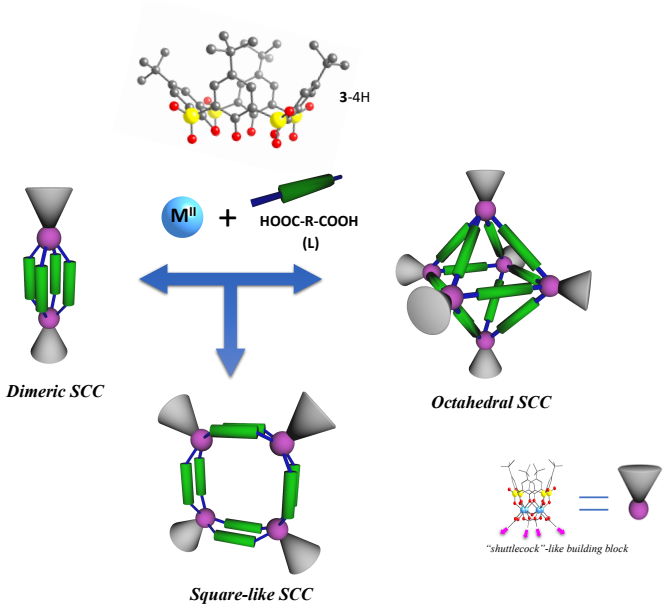

Figure 3. Formation of isomeric Supramolecular Coordination Cages (SCC) displaying different geometries and resulting from the three-components approach, by bridging "shuttlecock"-like $[\mathbf{3}\text{-}M_4(OH_2)]^{4+}$ building blocks based on tetranuclear clusters of tetrasulfonylcalix[4]arene $\mathbf{3}^{4-}$ with divalent cations M^{2+}, and V-shaped or linear dicarboxylic ditopic connectors L.

However, the use of conformationally flexible ditopic carboxylate compounds was not investigated, although it may lead to new supramolecular coordination cages able to adapt their inner *endo* cavity for accommodation of appropriate molecular guests. Moreover, a study of the use of flexible connectors for the formation of MOFs, was successfully demonstrated by the formation of new stimuli responsive MOFs resulting from the use of such flexible aliphatic linker leading to a generation of material exhibiting tunable gas adsorption properties.[61]

Herein we report on the synthesis and solid-state characterization of unique adaptative SCCs resulting from the three-components approach and the fusion of two tetranuclear or trinuclear tetrasulphonylcalix[4]arene based species by flexible succinic acid, in basic conditions, leading to hexanuclear and octanuclear nanosized containers respectively.

Results and discussion

The formation of three types of four nanocontainers is presented below, together with their structural description.

Description of achiral structure of $\mathbf{3_2Co_8(suc)_4}$

The slow liquid diffusion, of a MeOH solution of stochiometric quantity of triethyl amine (10 equivalents) as a base, into a DMF solution with dissolved metal (II) nitrate salt, **3**-4H and succinic acid mixed in molar ration 1/4/2, was used and led to the formation of two types of crystals differing by their colors and shapes (see experimental part).

The first one, slight rose needles, is the achiral compound $\mathbf{3_2Co_8(suc)_4}$, which can be described by the general formula

[$\mathbf{3}_2Co_8(OH_2)_2(suc)_4$]·2DMF. Compound $\mathbf{3_2Co_8(suc)_4}$ crystallizes in the centrosymmetric *P*-1 space group (see crystallographic table 1). This octanuclear complex is a neutral symmetrical dimeric compound (figure 4a) composed of two succinate moieties (suc^{2-}), one tetranuclear cluster based on $\mathbf{3}^{4-}$, one μ_4-H_2O molecule and one DMF uncoordinated molecule. Each calixarene moiety form *exo* cavity with located disordered solvate DMF molecule inside.

One tertiobutyl group belonging to $\mathbf{3}^{4-}$ is found to be disordered. The formation of the octanuclear complex appears as the fusion of two tetranuclear "shuttlecock"-like [$\mathbf{3}Co_4(OH_2)$]$^{4+}$ cationic units by the flexible succinate di-anion, leading to an adaptative symmetrical coordination "cage".

In the obtained neutral nanocontainers of $\mathbf{3_2Co_8(suc)_4}$, each Co^{2+} metallic centers adopt a deformed octahedral geometry, where the coordination sphere around the metallic centers is formed by two μ_2-phenoxo from $\mathbf{3}^{4-}$, one O from the sulfonyl groups of $\mathbf{3}^{4-}$, two oxygens from the succinate ligands, and one O from the μ_4-bridging water molecule, as frequently reported in the literature for similar systems.[62,63] The distances around the metallic centers are in accordance with the oxidation state +II of the metallic centers, as shown in table 2.

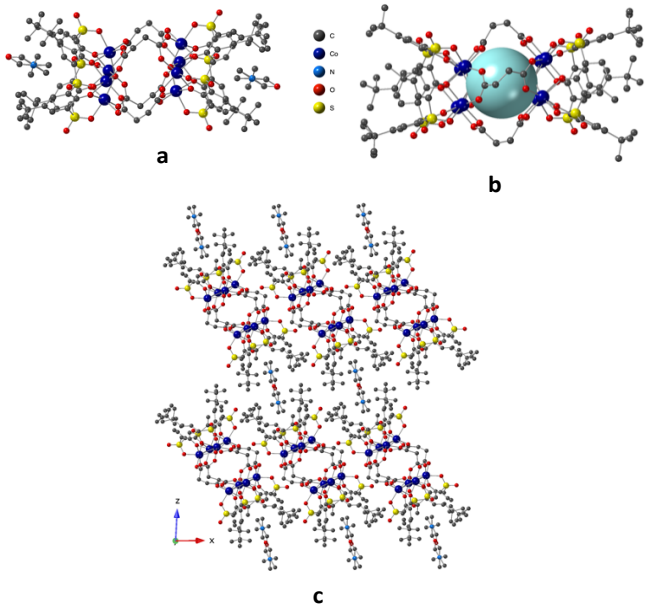

Figure 4. The structure of $\mathbf{3_2Co_8(suc)_4}$ obtained by X-Ray diffraction on single crystals: a) the different components with one disordered DMF molecule in the *exo* cavity b) the formed *endo* cavity of the nano-container and b) the packing of the complexes in the xOz plane. H atoms are omitted for clarity. For bond distances and angles see the text and Table 2.

The succinate ligands are slightly deformed and the diameter of the inner resulting *endo* cavity is *ca* 7Å, as shown in figure 4b.

The disordered DMF molecules located in the *exo* cavities are interacting with aromatic rings by CH- π weak interactions. The complexes are stacked together in ribbons along the *a* axis without any specific interactions, displaying face to face orientation of symmetrical calixarene *exo* cavities, as shown in figure 4c.

The crystallinity and phase purity of the as-synthesized materials were studied by the powder X-ray diffraction (PXRD), as shown in figure S1 (see SI). The analysis of the observed pattern revealed the presence of a mixture of two crystalline phases in the polycrystalline powder obtained in slow diffusion conditions.

Description of the isostructural chiral cages $\mathbf{3_2M_8(suc)_4}$-M (M = Co, Ni)

In order to establish the nature of the other crystalline phase observed while crystallizing $\mathbf{3_2Co_8(suc)_4}$, another crystal distinct from the first one, with an intense pink color and a prismatic shape, was analyzed using X-ray diffraction. It revealed the formation of a chiral complex composed of the same components as the one reported for $\mathbf{3_2Co_8(suc)_4}$, but differs by the presence of co-crystallized neutral species of formula $Co(OH)_2(DMF)_4$, giving rise to the complex of general formula [$\mathbf{3}_2Co_8(OH_2)_2(suc)_2)_4$]•$2Co(OH)_2(DMF)_4$•$2H_2O$•4DMF ($\mathbf{3_2Co_8(suc)_4}$**-Co**). Surprisingly the formation of the isomorphous analogue of $\mathbf{3_2Co_8(suc)_4}$**-Co** was observed when $Ni^{II}(NO_3)_2$ $6H_2O$ was mixed with succinic acid and **3**-4H under solvotermal conditions (see experimental part). It is important to note that the use of $Ni^{II}(NO_3)_2$ $6H_2O$ in comparable mild condition leads to a mixture of undefined compounds.

Both $\mathbf{3_2M_8(suc)_4}$**-M** compounds (M=Co or Ni) crystallizes in the non-centrosymmetric chiral $P4_22_12$ space group (see crystallographic table 1), with Flack parameter of -0.020(2) and 0.031(8) for M = Co and Ni, respectively, suggesting that the investigated single crystals are homochiral.

The independent part of $\mathbf{3_2M_8(suc)_4}$**-M** (M=Co or Ni) consists of $\mathbf{3_2M_8(suc)_4}$ complex, that is similar to one described above, two free water molecules and neutral $M^{II}(DMF)_4(OH)_2$ (M = Co or Ni) units, as shown in figures 5 a and b for M = Co and Ni respectively. In addition, for the Co complex, four DMF molecules located in calix[4]arene *exo* cavities were also refined in the unit cell. In the crystals of $\mathbf{3_2Co_8(suc)_4}$**-Co** and $\mathbf{3_2Ni_8(suc)_4}$**-Ni** some tertiobutyl groups and phenyl moieties of the macrocyclic fragments are also found to be disordered. Both compounds $\mathbf{3_2Co_8(suc)_4}$**-Co** and $\mathbf{3_2Ni_8(suc)_4}$**-Ni** are isomorphous but also solvates.

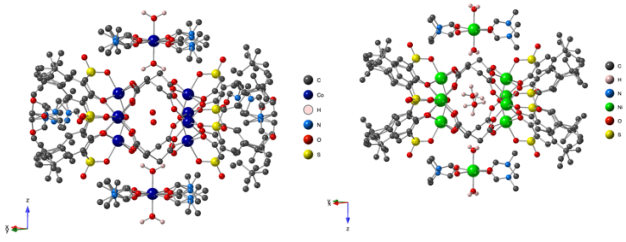

Figure 5. The general components, established by X-Ray diffraction on single crystals for a) $\mathbf{3_2Co_8(suc)_4}$**-Co** and b) $\mathbf{3_2Ni_8(suc)_4}$**-Ni**. H atoms are omitted for clarity (except those located on hydroxyl and, when possible, water molecules). For bond distances and angles see the text and Table 2.

As in the case of the previously described compound $\mathbf{3_2Co_8(suc)_4}$, compounds $\mathbf{3_2Co_8}$ **(suc)**$_4$**-Co** and $\mathbf{3_2Ni_8(suc)_4}$**-Ni**, are similar by the coordination environment and bond distances around the metallic centers coordinated to $\mathbf{3}^{4-}$ and in accordance with the oxidation state +II of Cobalt and Nickel atoms, as shown in table 2.

The presence of neutral $M^{II}(DMF)_4(OH)_2$ (M = Co or Ni) complexes (figure 6 a) in the unit cell appears very intriguing. Interestingly, this type of neutral Ni mononuclear species located in the unit cell of neutral SCC octahedral M_{24}-cage based on **3**-4H prepared in solvothermal conditions, has also been recently reported,[45] presenting Ni^{II}-OH distance of 1.988Å, whereas for **$3_2Ni_8(suc)_4$-Ni**, the Ni^{II}-OH distance was equal to 1.958(11). Another related isolated complex involving Co(II) ions was also reported, displaying Co^{II}-OH distance of 2.095Å, whereas for **$3_2Co_8(suc)_4$-Co**, it was found out the Co^{II}-OH distance equal to 2.011(6). This fact unambiguously indicates the presence of neutral complex $M^{II}(DMF)_4(OH)_2$ (M = Co or Ni) in **$3_2Co_8(suc)_4$-Co** and **$3_2Ni_8(suc)_4$-Ni**, formed in basic conditions during the self-assembly process.

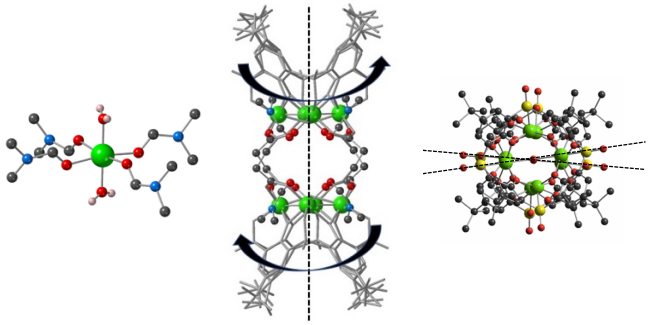

a **b** **c**

Figure 6. For **$3_2M_8(suc)_4$-M (M = Co or No),** a) the co-crystallized neutral $Ni^{II}(DMF)_4(OH)_2$ complex, b) the origin of chirality in **$3_2M_8(suc)_4$-M**, side view and c) top view of helical structure of **$3_2M_8(suc)_4$** unit screwed along the principal C_4 symmetry axis. H atoms are omitted for clarity (except those located on hydroxyl groups displaying disordered character).

It is worth noting that, in both compounds, there are no chiral centers in the starting components forming the crystals of **$3_2M_8(suc)_4$-M**, but the observed chirality arises (i) from the $M^{II}(DMF)_4(OH)_2$ (M = Co or Ni) complexes, by four screwed DMF around the M^{II}-cation (α chirality) and also (ii) from the conformational change within the **$3_2M_8(suc)_4$** unit imposed by the left-handed (or right-handed) screwed calixarene caps along the principal C_4 axis (figure 6b) of the opposite (**3**$M_4(OH_2)$) moieties leading to the overall helicate structure with the rotation angle equal to 11.2° (figure 6c).

As it was found out, the generation of this chiral structure is supported by formation of 1D H-bonded chain along the *c* axis, which occurs between M-OH moieties of the $M^{II}(DMF)_4(OH)_2$ complexes and the dimeric calixarene based units with the distances O_{suc}-$O_{M(OH)}$ of 2.734(5) and 3.178(5) Å for M = Co and 2.777(6) and 3.170(5) Å for M = Ni (figure 7a). All calixarene based building blocks located in the 1D H-bonded molecular architecture display the same induced left-handed (or right-handed) chirality, as shown in figure 7b. The H_2O molecules also interact with the carboxylate moieties through hydrogen bonding with O-O distances of 2.913(5) and 3.458(6) Å for M = Co and 2.931(5) and 3.432(5) Å for M = Ni, respectively. Despite of the conformational change within the structure of dimeric calixarene complex, the hydrophilic pockets in the *endo* cavities of the formed nano-containers displays practically the same diameter of *ca* 7Å as observed in **$3_2Co_8(suc)_4$** (figure 7a).

The formed chiral 1D supramolecular chains running along the *c* axis, are arranged in perpendicular fashion in the xOy plane in the unit cell, as shown in figure 7b.

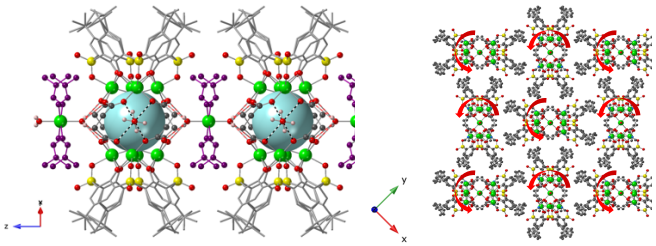

a **b**

Figure 7. For **$3_2Ni_8(suc)_4$-Ni** a) the 1D H-bonded chain formed in **$3_2Ni_8(suc)_4$-Ni**, together with the *endo* cavities of the nano-container, where H-bonds are represented in dashed lines. The coordinated DMF molecules are represented in violet. and b) the crystal packing of in the xOy plane showing the perpendicular stacking of 1D H-bonded chains. H atoms are omitted for clarity (except those located on hydroxyl and, when possible, water molecules). For bond distances and angles see the text and Table 2.

The crystallinity and phase purity of the as-synthesis Ni-based crystalline material were confirmed by the powder X-ray diffraction (PXRD) patterns, shown in figure S2 (see SI).

For **$3_2Ni_8(suc)_4$-Ni**, the TGA trace confirms the presence of $4H_2O$ and 4DMF molecules in the unit cell, as refined by XRD (figure S4, SI).

Description of the structure of $3_2Zn_6(suc)_2$

The combination of **3**-4H with $Zn^{II}(NO_3)_2 \cdot 6H_2O$ and succinic acid (**suc**-2H) in 1/4/2 molar ratio (**3**-4H/M/L) under solvothermal conditions afforded crystals of targeted Zn-based complex **$3_2Zn_6(suc)_2$** (see experimental part). The structural analysis revealed that it crystallizes in the centrosymmetric orthorhombic *P*bcn space group (see crystallographic table 1) giving rise to crystals of formula [**$3_2Zn_6(suc)_2$**$(OH_2)_2(DMF)_4$]•10 DMF). It should be noted that, contrary to the previously described **$3_2Co_8(OH_2)_2(suc)_4$** synthesis, the use of slow liquid diffusion techniques leads to the formation of crystals of initial calixarene complex with NEt_3.

As confirmed by the X-ray diffraction on single crystal, **$3_2Zn_6(suc)_2$** is composed of two tetradeprotonated calixarene moieties $\mathbf{3}^{4-}$, each coordinated to three divalent zinc cations forming two clusters connected by two deprotonated succinate anions (suc^{2-}), as shown in figure 8a. Besides, one molecule of water laying in the center of the trinuclear clusters in the common vertices of the formed Zn^{II} octahedrons and four DMF molecules complete the coordination spheres of Zn-atoms. In the crystal, one can also find ten others disordered DMF molecules and among them, one is present in the *exo* hydrophobic cavity of the calixarene moiety, with weak CH-π interactions.

This hexanuclear (**3**$Zn_3(OH_2)(suc)(DMF)_2)_2$ complex is symmetrical and neutral and presents a center of symmetry located in the middle of the *endo* cavity. One tertiobutyl group belonging to $\mathbf{3}^{4-}$ is found to be disordered.

The succinate ligands are deformed and the diameter of the inner cavity is decreased to *ca* 5Å, as shown in figure 8b, compared to the one reported in three related compounds.
In the neutral complex, the Zn atoms are in deformed octahedral geometries, with Zn-O distances shown in table 2 accounting for a +II oxidation state of Zn.

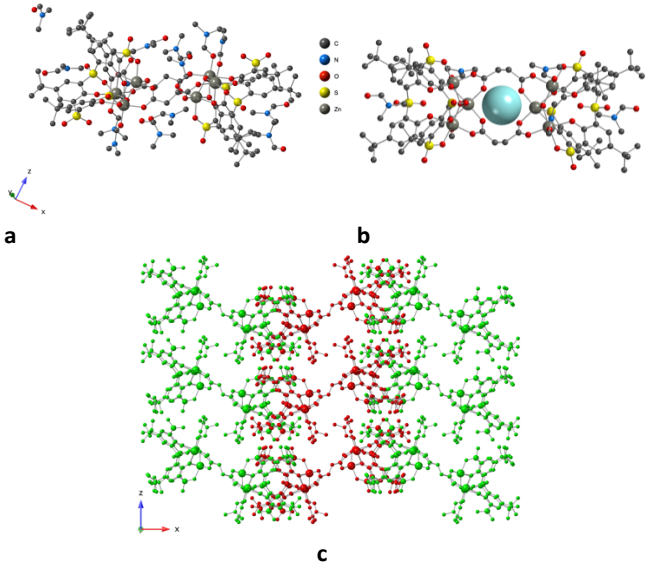

Figure 8. The structure of **$3_2Zn_6(suc)_2$** obtained by X-Ray diffraction on single crystals: a) the different components and b) the *endo* cavities of the nano-container and c) the packing of the clusters in the xOz plane. H atoms are omitted for clarity. For bond distances and angles see the text and Table 2.

In the crystal, the complexes are stacked parallelly along the *c* axis, as shown in figure 8c, forming interpenetrated ribbons, with free DMF molecules located in the interstices.

The crystallinity and phase purity of the as-synthesis materials were confirmed by the powder X-ray diffraction (PXRD) patterns, shown in figure S3 (see SI), demonstrating the good match of XRPD patterns between experimental diffractogram and simulated one obtained from single crystal X-ray diffraction.

For **$3_2Zn_6(suc)_2$**, the TGA trace confirm the presence of $2H_2O$ and 7 DMF molecules (figure S4, SI).

Discussion

As it was demonstrated, the use of flexible succinic acid for the building of Supramolecular Coordination Cages based on **3**-4H, led to four coordination compounds of three different types. In all cases, the polynuclear clusters, "shuttlecock"-like building blocks containing three or four metallic cations in the cluster core, are found in the supramolecular entities of general formula (**3**M_x(**suc**)$_y$)$_2$ (M = Co and Ni, **suc** is the succinate ligand, x = 3 or 4, y = 1 or 2).
Despite using analogous starting compounds for the synthesis, the three types of observed SCCs are: 1) symmetrical achiral Co_8-cage built from two tetranuclear clusters fused by four succinate linkers (**$3_2Co_8(suc)_4$**), 2) chiral M_8-cage (M = Co, Ni) composed of two tetranuclear moieties connected by four succinate linkers (**$3_2Co_8(suc)_4$-Co, $3_2Ni_8(suc)_4$-Ni**) and 3) achiral symmetrical Zn_6-cage resulting from interaction of two trinuclear clusters *via* two succinate ligands (**$3_2Zn_6(suc)_2$**) (figure 9).

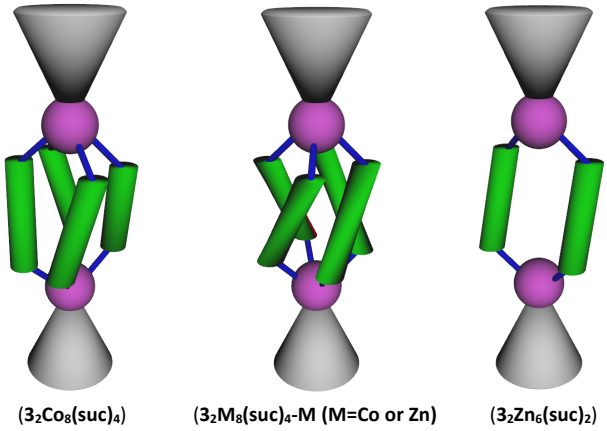

Figure 9. Schematic representation of the three types of obtained SCCs.

Indeed, the flexibility of succinate linkers as well as the nature of the used transition metal cations play the crucial role in the formation sulfonylcalix[4]arene based SCCs. The evaluation of the torsion angles of the CH_2 groups in the carbon chain of succinate ligand and their mutual orientations is also indicating the flexibility of the used ligand and the consequence of this is the size of the *endo* cavities of the formed nanocontainers (table 3).

Table 3. Torsion angle in the succinic linker and the size of endo cavities observed for obtained supramolecular compounds.

	$3_2Co_8(suc)_4$	$3_2Co_8(suc)_4$-Co	$3_2Ni_8(suc)_4$-Ni	$3_2Zn_6(suc)_2$
	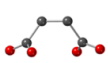	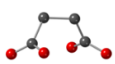	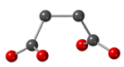	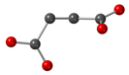
Torsion angle (°)	±61.6 (9), ±69.8 (8)	+(-)61.2 (5)	+(-)59.3 (9)	+90.7 (7) -103.6 (7)
Size of *endo* cavity (Å)	7	7	7	5

Unfortunately, for Co-based compounds (**$3_2Co_8(suc)_4$** and **$3_2Co_8(suc)_4$-Co**), it was not possible to determine the experimental conditions to shift the equilibrium to one of both compounds, whereas the use of Ni^{II} cations in solvothermal conditions led to formation of only one crystalline phase that presumably is related with interplay of thermodynamic and the kinetic factors affecting on the equilibrium in the complex multicomponent Co and Ni based supramolecular systems.
Concerning the use of Zn^{II} cations, the nuclearity of the obtained complexes appears to be controlled also by different factors, but the most important can be related to the particular affinity of the Zn^{II} cations to form trinuclear Zn(II) species when coordinated to tetrasulfonylcalix[4]arene[62,63] and thiacalix[4]arene, as already observed.[64]

If achiral complexes **$3_2Co_8(suc)_4$** and **$3_2Zn_6(suc)_2$** contain both left-handed as well as right-handed succinic moieties in the complex structure, for chiral **$3_2Co_8(suc)_4$-Co** and **$3_2Ni_8(suc)_4$-Ni** compounds, only one type (left-handed or right-handed) of succinic moieties is present in the unit cell. The formation of chiral nanosized cages based on calixarene and on tetrasulfonylcalix[4]arene has been scarcely reported in the literature: one example for the formation of octahedral M_{24} cages has been provided[53] and for the formation of M_8 cages examples have been reported stating from a chiral ditopic ligand.[57] Although the case of induced chirality in the crystalline state, starting from achiral compounds has been well documented in the literature,[65,66,67] this work presents the first example of the formation of chiral crystalline coordination compounds resulting from the H-bonding between the two different components: metal-calixarene based nanocontainers and $M^{II}(DMF)_4(OH)_2$ neutral species.

Conclusions

In this work, the formation of adaptative metal-organic nanocontainers or Supramolecular Coordination Cages using the three components approach based on tetrasulfonylcalix[4]arene (**3**-4H), metallic salts and flexible succinic acid as organic linker, was demonstrated. As a result, the generation of four new SCCs of three different types, displaying dimeric-like structures and differing by the number of involved metallic centers and conformational behavior of succinic acid moieties, have been observed in the crystalline phase. All obtained compounds have been characterized from a structural point of view using X ray diffraction on single crystal and powder, when possible. Among them, two complexes **$3_2Co_8(suc)_4$** and **$3_2Zn_6(suc)_2$** represent the achiral symmetrical species, whereas for others two isomorphous compounds **$3_2M_8(suc)_4$-M** (M = Co or Ni) where induced chirality involving the hydrogen bonding between the initially achiral crystal components was observed. It was shown that the crystal structure of the obtained coordination compounds depends of the nature of the used metallic cation, number of flexible organic linkers and the presence of co-crystallized $M^{II}(DMF)_4(OH)_2$ neutral species within the unit cell.

For obtained chiral nanocontainers, applications in the field of enantiomeric separation, recognition of chiral molecular compounds and asymmetric catalysis is currently under investigation.

In addition, the use of tetrasulfonylcalix[4]arene building blocks when combined with other flexible organic polycarboxylate linkers containing for example longer carbon chain or additional chiral centers encored within the linker framework is expected to be a powerful tool to construct new functional adaptative supramolecular nano-containers.

Experimental

Synthesis

Tetrasulphonylcalix[4]arene **3**-4H were synthesized following the earlier described procedure.[13] All solvents and reagents used for the synthesis were of analytical grade and used without further purification. Succinic acid, nitrate salts of nickel (II) and cobalt (II) were purchased from Sigma-Aldrich (Darmstadt, Germany).

$3_2Co_8(suc)_4$* and *$3_2Co_8(suc)_4$-Co

At RT, in a crystallization tube (diameter 12 mm and height 12 cm) a clear DMF solution (4 ml) containing **3**-4H (30 mg, 0.035 mmol) succinic acid (8 mg, 0.07 mmol) and $Co(NO_3)_2 \bullet 6H_2O$ (40 mg, 0.14 mmol) was deposited, upon which a DMF/MeOH mixture (1/1, 2 ml) was layered. Then, a solution of NEt_3 (0.05 ml, 0.35 mmol) in MeOH (4 ml) was slowly added. A liquid diffusion at the room temperature produced single-crystals suitable for X-ray diffraction after 2 weeks. As attested by XRPD analysis, the obtained crystalline phase was composed of only two phases including to **$3_2Co_8(suc)_4$** (slight rose needles) and **$3_2Co_8(suc)_4$-Co** (intense pink prisms).

$3_2Ni_8(suc)_4$-Ni

In a Pyrex crystallization reactor equipped with a screw cap, **3**-4H (30 mg, 0.035 mmol), succinic acid (8 mg, 0.07 mmol) and $Ni(NO_3)_2 \bullet 6H_2O$ (40 mg, 0.14 mmol) were dissolved in a DMF/MeOH solution (1/1, 10 ml). Then, the solution was heated under MW irradiation conditions (100 W) and stirred for 4 hours. After cooling and filtration, green single crystals suitable for X-ray diffraction analysis were obtained upon slow evaporation of the mother liquor at room temperature in 7 days. Total yield: 45 mg (42 %, according to ligand **3**-4H). Anal. Found for $C_{108}H_{138}N_4O_{50}S_8Ni_9$: C, 42.16; H, 4.52; N, 1.82 %. Calc. C, 43.20; H, 4.68; N, 2.05 %. IR (KBr, cm^{-1}) υ: 3438 (m), 2962 (s), 1668 (m), 1607 (s), 1494 (s), 1454 (s), 1292 (s), 1264 (s), 1137 (m), 1084 (s), 906 (m), 841 (m), 801 (s), 627 (m), 569 (s), 488 (m). (see figure S5, ESI).

$3_2Zn_6(suc)_2$

The same procedure, as described for **$3_2Ni_8(suc)_4$-Ni**, was applied, using $Zn(NO_3)_2 \bullet 6H_2O$ instead of $Ni(NO_3)_2 \bullet 6H_2O$ salt. The colorless crystals were formed in 9 days after cooling and filtration of the mother liquor. Total yield: 60 mg (50 %, according to ligand **3**-4H). Anal. Found for $C_{130}H_{196}N_{14}O_{48}S_8Zn_6$: C, 46.31; H, 5.86; N, 5.82%. Calc. C, 46.75; H, 5.95; N, 5.92 %. IR (KBr, cm^{-1}) υ: 3442 (m), 2961 (s), 2923 (s), 1656 (s), 1606 (s), 1537 (s), 1493 (s), 1452 (s), 1401 (m), 1290 (m), 1264 (m), 1134 (m), 1083 (s), 799 (m), 625 (m), 561 (s). (see figure S5, ESI).

Characterization techniques

Elemental analysis was performed on a Vario Macro CHN Analyzer (Elementar Analysensysteme GmbH, Langenselbold, Germany).

Infrared spectra (IR) of milled crystalline samples in KBr were recorded on a Tensor 27 Fourier-transform spectrometer (Bruker) in a range of 4000-400 cm^{-1} with an optical resolution of 4 cm^{-1} and an accumulation of 32 scans.

Single-Crystal X-ray diffraction

Data set for single crystals **$3_2Co_8(suc)_4$-Co** was collected on a Rigaku XtaLab Synergy S instrument with a HyPix detector and a PhotonJet microfocus X-ray tube using Cu-Kα (1.54184 Å) radiation at 100 K. Images were indexed and integrated using the CrysAlisPro data reduction package. Data were corrected for systematic errors and absorption using the ABSPACK module. The GRAL module was used for analysis of systematic absences and space group determination. Using the Olex 2 software,[68] structure was solved by direct methods with SHELXT[69] and refined by the full-matrix least-squares on F^2 using SHELXL.[70] Non-hydrogen atoms were refined anisotropically. Absolute configuration of **$3_2Co_8(suc)_4$-Co** was established by anomalous-dispersion effects in diffraction measurements on the crystal. DMF molecule and tert-butyl fragments were disordered over two positions. DMF molecules were located with the aid of Ilia's Fragment Library[71] and subsequently refined with constraints and restraints.

Diffraction data for single-crystals of **$3_2Ni_8(suc)_4$-Ni**, **$3_2Co_8(suc)_4$** and **$3_2Zn_6(suc)_2$** were collected at 100 K on the 'Belok/XSA' beamline (λ = 0.79370 Å, ϕ-scans) of the Kurchatov Synchrotron Radiation Source (Moscow, Russian Federation).[72,73] Diffraction patterns were collected using Mardtb goniometer equipped with Rayonix SX165 2D positional sensitive CCD detector at 100 K. In total, 300 frames were collected with oscillation range of 1°. The data were indexed, integrated and scaled, absorption correction was applied using the XDS program package.[74] The structures were solved by direct methods with software SHELXT.[69] The structural model was investigated and refined by using Olex 2 software[68] by a full-matrix least-squares method on F^2 with anisotropic displacement. All hydrogen atoms were placed in calculated positions and included in the refinement within the riding model with fixed isotropic displacement parameters Uiso(H) = 1.5Ueq(O), 1.2Ueq(N), and 1.2Ueq(C).

Crystallographic Data Centre via www.ccdc.cam.ac.uk/datarequest/cif. CCDC: **$3_2Co_8(suc)_4$**: 2116175; **$3_2Co_8(suc)_4$-Co**: 2116177; **$3_2Ni_8(suc)_4$-Ni**: 2116176 and **$3_2Zn_6(suc)_2$**: 2116178.

X-ray diffraction on powder

Powder diffraction studies (PXRD) diagrams were collected on polycrystalline samples at the room temperature (293(2) K), on a Bruker D8 diffractometer using monochromatic Cu-Kα radiation with a scanning range between 2° and 40° at a scan step size of 2° min^{-1}.

TGA measurements

A TG/DSC NETZSCH (Selb, Germany) STA449 F3 were used for the thermal analysis (thermogravimetry/differential scanning calorimetry) in which the variation of the sample mass as a function of temperature and the corresponding heats are recorded. An approximately 15 mg sample was placed in an Al crucible with a pre-hole on the lid and heated from 25 to 500°C. The same empty crucible was used as the reference sample. High-purity argon was used with a gas flow rate of 50mL/min. TGA measurement were performed at the heating rates of 5 K/min.

Author Contributions

All authors contributed equitably to the final manuscript.

Conflicts of interest

"There are no conflicts to declare".

Acknowledgements

This work was supported by Russian Science Foundation (project № 19-73-20035). The authors are grateful to Kurchatov Institute for performing of XRD-analysis, to Spectral-Analytical Center of FRC Kazan Scientific Center of RAS for their help and support in TGA, PXRD and IR studies. Ayrat R. Khamatgalimov is warmly acknowledged for TGA measurements. D.I., A.G., A.S. acknowledge the support by the Government assignment for FRC Kazan Scientific Center of RAS. Financial support from the University of Strasbourg, the Institute Universitaire de France and the CNRS are also acknowledged.

Notes and references

1 Y.-Y. Zhang, W.-X. Gao, L. Lin, G.-X. Jin, Recent advances in the construction and applications of heterometallic macrocycles and cages. *Coord. Chem. Rev.* **2017**, *344*, 323-344.

2 A. E. Martín Díaz, J.E.M. Lewis, Structural Flexibility in Metal-Organic Cages. *Front. Chem.* **2021**, *9*, 706462.

3 M. Han, D.M. Engelhard, G.H. Clever, Self-assembled coordination cages based on banana-shaped ligands. *Chem. Soc. Rev.* **2014**, *43*, 1848-1860.

4 A.J. Gosselin, C.A. Rowland, E.D. Bloch, Permanently Microporous Metal–Organic Polyhedra. *Chem. Rev.* **2020**, *120*, 16, 8987-9014.

5 N. Hosono, S. Kitagawa, Modular Design of Porous Soft Materials via Self-Organization of Metal–Organic Cages. *Acc. Chem. Res.* **2018**, *51*, 2437-2446.

6 F.J. Rizzuto, L.K.S. von Krbek, J.R. Nitschke, Strategies for binding multiple guests in metal–organic cages. *Nat. Rev. Chem*. **2019**, *3*, 204-222.

7 E.G. Percástegui, T.K. Ronson, J.R. Nitschke, Design and Applications of Water-Soluble Coordination Cages. *Chem. Rev.* **2020,** *120,* 24,13480-13544.

8 I S Antipin *et al.*, Functional supramolecular systems: design and applications. *Russ. Chem. Rev*. **2021**, *90*, 8, 895-1107.

9 L. He, S.-C. Wang, L.-T. Lin, J.-Y. Cai, L. Li, T.-H. Tu, Y.-T. Chan. Multicomponent Metallo-Supramolecular Nanocapsules Assembled from Calix[4]resorcinarene-Based Terpyridine Ligands. *J. Am. Chem. Soc.* **2020**, *142*, 15, 7134-7144.

10 X. Hu, M. Han, L. Shao, C. Zhang, L. Zhang, S. P. Kelley, C. Zhang, J. Lin, S.J. Dalgarno, D.A. Atwood, S. Feng, J.L. Atwood. Self-Assembly of a Semiconductive and Photoactive

Heterobimetallic Metal–Organic Capsule, *Angew. Chem. Int. Ed.,* **2021**, *60*, 10516-10520.
11 C. D. Gutsche, in Calixarenes Revised: Monographs in Supramolecular Chemistry Vol. 6, The Royal Society of Chemistry, Cambridge, **1998**.
12 H. Kumagai, M. Hasegawa, S. Miyanari, Y. Sugawa, Y. Sato, T. Hori, S. Ueda, H. Kamiyama, S. Miyano, Facile synthesis of p-tert-butylthiacalix[4]arene by the reaction of p-tert-butylphenol with elemental sulfur in the presence of a base. *Tetrahedron Lett.,* **1997**, *38*, 3971-3971.
13 N. Iki, H. Kumagai, N. Morohashi, K. Ejima, M. Hasegawa, S. Miyanari, S. Miyano, Selective oxidation of thiacalix[4]arenes to the sulfinyl- and sulfonylcalix[4]arenes and their coordination ability to metal ions. *Tetrahedron Lett*. **1998**, *39*, 7559-7562.
14 G. Mislin, E. Graf, M.W. Hosseini, A. De Cian, Sulfone-calixarenes: a new class of molecular building block. *Chem. Commun*, **1998**, 1345-1346.
15 T. Kajiwara, N. Iki, M. Yamashita, Transition metal and lanthanide cluster complexes constructed with thiacalix[n]arene and its derivatives. *Coord. Chem. Rev*. **2007**, *251*, 1734-1746.
16 B. S. Creavena, D. F. Donlona, J. McGinley Coordination chemistry of calix[4]arene derivatives with lower rim functionalisation and their applications. *Coord. Chem. Rev*. **2009**, *253*, 893-962.
17 J. P. Chinta, B. Ramanujam, C.P. Rao Structural aspects of the metal ion complexes of the conjugates of calix[4]arene: Crystal structures and computational models. *Coord. Chem. Rev.* **2012**, *256*, 2762-2794.
18 R. Kumar, Y. O. Lee, V. Bhalla, M. Kumar, J. S. Kim, Recent developments of thiacalixarene based molecular motifs. *Chem. Soc. Rev*. **2014**, *43*, 4824-4870.
19 R. O. Fuller, G. A. Koutsantonis, Magnetic properties of calixarene-supported metal coordination clusters. *Coord. Chem. Rev*. **2020**, 402, 213066.
20 T. Kajiwara, K. Katagiri, M. Hasegawa, A. Ishii, M. Ferbinteanu, S. Takaishi, T. Ito, M. Yamashita, N. Iki, Conformation-Controlled Luminescent Properties of Lanthanide Clusters Containing p-tert-Butylsulfonylcalix[4]arene. *Inorg. Chem*. **2006**, *45*, 4880-4882.
21 C.-Z. Sun, L.-Y. Zhang, J.-Y. Wang, Z.-N. Chen, F.-R. Dai, Sensitive and selective urinary 1-hydroxypyrene detection by dinuclear terbium-sulfonylcalixarene complex. *Dalton Trans.* **2018**, *47*, 8301-8306.
22 C.-M. Liu, D.-Q. Zhang, X. Hao, D.-B. Zhu, Syntheses, Crystal Structures, and Magnetic Properties of Two p-tert-Butylsulfonylcalix[4]arene Supported Cluster Complexes with a Totally Disordered Ln4(OH) 4Cubane Core. *Cryst. Growth Des*. **2012**, *12*, 2948-2954.
23 T. Kajiwara, H. Wu, T. Ito, N. Iki, S.Miyano, Octalanthanide Wheels Supported by p-tert-Butylsulfonylcalix[4]arene, *Angew. Chem. Int. Ed.* **2004**, *43*, 1832-1835.
24 T. Kajiwara, K. Katagiri, S. Takaishi, M. Yamashita, N. Iki, Dodecalanthanide Wheel Supported by p-tert-Butylsulfonylcalix[4]arene. *Chem. Asian J.* **2006**, *1*, 349-351.
25 K. Su, F. Jianga, M. Wu, J. Qian, J. Pang, D. Yuan, M. Hong, Syntheses, structures, luminescent and magnetic properties of three high-nuclearity neodymium compounds based on mixed sulfonylcalix[4]arene-phosphonate ligands. *CrystEngComm*. **2016**, *18*, 4921-4928.
26 N. O'Toole, C. Lecourt, Y. Suffren, A. Hauser, L. Khrouz, E. Jeanneau, A. Brioude, D. Luneau, C. Desroches, Photogeneration of Manganese(III) from Luminescent Manganese(II) Complexes with Thiacalixarene Ligands: Synthesis, Structures and Photophysical Properties, *Eur. J. Inorg. Chem.* **2019**, 73-78.
27 G. Desroches, G. Pilet, P.A. Szilagyi, G. Molnar, S.A. Borshch, A. Bousseksou, S. Parola, D. Luneau, Tetra- and Decanuclear Iron(II) Complexes of Thiacalixarene Macrocycles: Synthesis, Structure, Mössbauer Spectroscopy and Magnetic Properties *Eur. J. Inorg. Chem.*, **2006**, 357-365.
28 G. Karotsis, S.J. Teat, W. Wernsdorfer, S. Piligkos, S.J. Dalgarno, E.K. Brechin, Calix[4]arene-Based Single-Molecule Magnets, *Angew. Chem. Int. Ed.* **2009**, 48, 8285-8288.
29 M. Lamouchi, E. Jeanneau, A. Pillonnet, A. Brioude, M. Martini, O. Stéphan, F. Meganem, G. Novitchi, D. Luneau, C. Desroches, Tetranuclear manganese(II) complexes of sulfonylcalix[4]arene macrocycles:synthesis, structure, spectroscopic and magnetic properties, *Dalton Trans*., **2012**, *41*, 2707-2713.
30 M. Lamouchi, , E. Jeanneau, G. Novitchi, D. Luneau, A. Brioude, C. Desroches, Polynuclear Complex Family of Cobalt(II)/Sulfonylcalixarene: One-Pot Synthesis of Cluster Salt [Co14II]+[Co4II]- and Field-Induced SlowMagnetic Relaxation in a Six-Coordinate Dinuclear Cobalt(II)/ Sulfonylcalixarene Complex. *Inorg. Chem*. **2014**, *53*, 63-72.
31 R.O. Fuller, G.A. Koutsantonis, I. Lozića, M.I. Ogden, B.W. Skelton Manganese–calcium clusters supported by calixarenes. *Dalton Trans*., **2015**, *44*, 2132-2137.
32 Y. Suffren, N. O'Toole, A. Hauser, E. Jeanneau, A. Brioude C. Desroches Discrete polynuclear manganese(II) complexes with thiacalixarene ligands: synthesis, structures and photophysical properties. *Dalton Trans.*, **2015**, *44*, 7991-8000.
33 R.O. Fuller, G.A. Koutsantonis, M.I. Ogden, Magnetic properties of calixarene-supported metal coordination clusters, *Coord. Chem. Rev.* **2020**, *402*, 213066.
34 Y. Jiao, S. Sarwar, S. Sanz, J. van Leusen, N.V. Izarova, C.L. Campbell, E. K. Brechin, S.J. Dalgarno, P. Kögerler, Exploiting complementary ligands for the construction of square antiprismatic monometallic lanthanide SMMs, *Dalton Trans.* **2021**, *50*, 9648-9654.
35 A. Ovsyannikov, S. Solovieva, I. Antipin, S. Ferlay Coordination Polymers based on calixarene derivatives: Structures and properties. *Coord. Chem. Rev.* **2017**, *352*, 151-186.
36 C.-M. Liu, D.-Q. Zhang, X. Hao, D.-B. Zhu, Calixarene-Supported Polynuclear Cobalt(II) Cluster Complexes Tuned by Substitution Groups of the Second Bridging Ligands, *Eur. J. Inorg. Chem.* **2012**, 4210-4217,
37 G. Zhang, X. Zhu, M. Liu, W. Liao, A window frame-like square constructed by bridging Co4-(TC4A-SO2)-SBUs with 1,3-bis(2H-tertazol-5-yl)benzene, *J. Mol. Struct.* **2018**, *1151*, 29-33.
38 Y. Bi, S. Du, W. Liao, Thiacalixarene-based nanoscale polyhedral coordination cages. *Coord. Chem. Rev*. **2014**, *276*, 61-72.
39 K. Su, F. Jiang, J. Qian, Y. Gai, M. Wu, Salem M. Bawaked, S. M. Mokhtar, A. Al-Thabaiti, M. Hong, Generalized Synthesis of Calixarene-Based High-Nuclearity M4n Nanocages (M = Ni or Co n = 2-6). *Cryst. Growth Des*. **2014**, *14*, 3116-3123.
40 K. Su, F. Jiang, J. Qian, J. Pan, J. Pang, X. Wan, F. Hu, M. Hong, Self-assembly of two high-nuclearity manganese calixarene-phosphonate clusters: diamond-like Mn16 and drum-like Mn14. *RSC Adv*., **2015**, *5*, 33579-33585.
41 T. Kajiwara, T. Kobashi, R. Shinagawa, T. Ito, S. Takaishi, M. Yamashita, N. Iki, Highly Symmetrical Tetranuclear Cluster Complexes Supported by p-tert-Butylsulfonylcalix[4]arene as a Cluster-Forming Ligand. *Eur. J. Inorg. Chem*. **2006**, 1765-1770.
42 C.-Z. Sun, L.-J. Cheng, Y. Qiao, L.-Y. Zhang, Z.-N. Chen, F.-R. Dai, W. Lin, Z. Wang, Stimuli-Responsive Metal-Organic Supercontainers as Synthetic Proton Receptors. *Dalton Trans*. **2018**, *47*, 10256-10263.

43 F-R. Dai, D. C. Becht, Z. Wang, Modulating guest binding in sulfonylcalixarene-based metal–organic supercontainers *Chem. Commun*., **2014**, 50, 5385-5387.

44 Yao Jin, Hong Jiang, Xianhui Tang, Wenqiang Zhang, Yan Liu,Yong Coordination-driven self-assembly of anthraquinone-based metal–organic cages for photocatalytic selective [2 + 2] cycloaddition *Dalton Trans.***, 2021**, *50*, 8533-8539.

45 M. R. Dworzak, M. M. Deegan, G. P. A. Yap, E. D. Bloch Synthesis and Characterization of an Isoreticular Family of Calixarene-Capped Porous Coordination Cages *Inorg. Chem.* **2021**, *60*, 5607-5616.

46 F-R. Dai, Z. Wang, Modular Assembly of Metal–Organic Supercontainers Incorporating Sulfonylcalixarenes *J. Am. Chem. Soc*. **2012**, *134*, 8002-8005.

47 F-R. Dai, U. Sambasivam, A. J. Hammerstrom, Z. Wang, Synthetic Supercontainers Exhibit Distinct Solution versus Solid State Guest-Binding Behavior *J. Am. Chem. Soc*. **2014**, *136*, 7480-7491.

48 S. Du, T.-Q. Yu, W. Liao, C. HuStructure modeling, synthesis and X-ray diffraction determination of an extra-large calixarene-based coordination cage and its application in drug delivery. *Dalton Trans*. **2015**, *44*, 14394-14402.

49 S. Wang, X. Gao, X. Hang, X. Zhu, H. Han, W. Liao, W. Chen, Ultrafine Pt Nanoclusters Confined in a Calixarene-Based {Ni24} Coordination Cage for High-efficient Hydrogen Evolution Reaction. *J. Am. Chem. Soc.* **2016**, *138*, 50, 16236-16239

50 Y. Fang, Z. Xiao, J. Li, C. Lollar, L. Liu, X. Lian, S. Yuan, S. Banerjee, P. Zhang, H-C. Zhou, Formation of a Highly Reactive Cobalt Nanocluster Crystal within a Highly Negatively Charged Porous Coordination Cage *Angew. Chem. Int. Ed.*, **2018**, *57*, 5283-5287.

51 Y. Fang, X. Lian, Y. Huang, G. Fu, Z. Xiao, Q. Wang, B. Nan, J-P. Pellois, H-C. Zhou, Investigating Subcellular Compartment Targeting Effect of Porous Coordination Cages for Enhancing Cancer Nanotherapy *Small*, **2018**, *14*, 1802709.

52 W. Gong, D. Chu, H. Jiang, X. Chen, Y. Cui, Y. Liu, Permanent porous hydrogen-bonded frameworks with two types of Brønsted acid sites for heterogeneous asymmetric catalysis *Nat. Commun.,* **2019**, *10***,** 600.

53 C. Tan, J. Jiao, Z. Li, Y. Liu, X. Han, Y. Cui Design and Assembly of a Chiral Metallosalen-Based Octahedral Coordination Cage for Supramolecular Asymmetric Catalysis. *Angew. Chem. Int. Ed.* **2018**, *57*, 2085-2090.

54 F.-R. Dai, Y. Qiao, Z. Wang, Designing structurally tunable and functionally versatile synthetic supercontainers. *Inorg. Chem. Front*. **2016**, *3*, 243-249.

55 Y. Qiao, L. Zhang. J. Li, W. Lin, Z. Wang, Switching on Supramolecular Catalysis via Cavity Mediation and Electrostatic Regulation *Angew. Chem. Int. Ed.* **2016**, *55*, 12778-12782.

56 L-J. Cheng, X-X. Fan, Y-P. Li, Q-H. Wei, F-R. Dai, Z-N. Chen, Z. Wang, Engineering solid-state porosity of synthetic supercontainers via modification of *exo*-cavities *Inorg. Chem. Comm.*, **2017**, *78*, 61-64.

57 K. Su, F. Jiang, J. Qian, J. Pang, F. Hu, S.M. Bawaked, M. Mokhtar, S.A. Al-Thabaitic, M. Hong, Bridging different Co4–calix[4]arene building blocks into grids, cages and 2D polymers with chiral camphoric acid. *CrystEngComm*, **2015**, *17*, 1750-1753.

58 N. Bhuvaneswari, F.-R. Dai, Z.-N. Chen, Sensitive and Specific Guest Recognition via Pyridinium-Modification in Spindle like Coordination Containers, *Chem. Eur. J*. **2018**, *24*, 6580-6585.

59 N. Bhuvaneswari, K. P. Annamalai, F.-R. Dai, Z.-N. Chen, Pyridinium Functionalized Coordination Containers as a Highly Efficient Electrocatalyst for Sustainable Oxygen Evolution. *J. Mater. Chem. A* **2017**,*5*, 23559-23565.

60 C.-Z. Sun, T.-P. Sheng, F.-R. Dai, Z.-N. Chen, Sulfonylcalixaren-Based ortho-Dicarboxylate-Bridged Coordination Containers for Guest Encapsulation and Separation. *Cryst. Growth Des*. **2019**, 19, 1144-1148.

61 S. Wang, N. Xhaferaj, M. Wahiduzzaman, K. Oyekan, X. Li, K. Wei, B. Zheng, A. Tissot, J. Marrot, W. Shepard, C. Martineau-Corcos, Y. Filinchuk, K. Tan, G. Maurin, C. Serre, Engineering Structural Dynamics of Zirconium Metal–Organic Frameworks Based on Natural C4 Linkers. *J. Am. Chem. Soc.* **2019**, *141*, 17207−17216.

62 M. V. Kniazeva, A. S. Ovsyannikov, D. R. Islamov, A. I. Samigullina, A. T. Gubaidullin, S. E. Solovieva, I. S. Antipin, S. Ferlay, Formation of Unsymmetrical Trinuclear Metallamacrocycles Based on Two Different Cone Calix[4]arene Macrocyclic Rings. *Crystals*, **2020**, *10*, 364.

63 M. V. Kniazeva, A. S. Ovsyannikov, D. R. Islamov, A. I. Samigullina, A. T. Gubaidullin, P. V. Dorovatovskii, S. E. Solovieva, I. S. Antipin, S. Ferlay, Nuclearity control in calix[4]arene-based zinc(ii) coordination complexes. *CrystEngComm*, **2020**, *22*, 7693-7703.

64 A. Bilyk, A.K. Hall, J.M. Harrowfield, M.W. Hosseini, G. Mislin, B.W. Skelton, C. Taylor, A.H. White, Linear, Divergent Molecular Receptors – Subtle Effects of Transition Metal Coordination Geometry. *Eur. J. Inorg. Chem*., **2000**, 823-826.

65 W-G. Lu, J-Z. Gu, L. Jiang, M-Y. Tan, T-B. Lu Achiral and Chiral Coordination Polymers Containing Helical Chains: The Chirality Transfer Between Helical Chains *Cryst. Growth Des*. **2008**, *08*, 192-199.

66 T. Sasaki, Y. Ida, I. Hisaki, S. Tsuzuki, N. Tohnai, G. Coquerel, H. Sato, M. Miyata, Construction of Chiral Polar Crystals from Achiral Molecules by Stacking Control of Hydrogen-Bonded Layers Using Type II Halogen Bonds. *Cryst. Growth Des*. **2016**, *16*, 1626-1635.

67 Y-L. Gao, K. Y. Maryunina, S. Hatano, S. Nishihara, K. Inoue, M. Kurmoo, Co-Crystallization of Achiral Components into Chiral Network by Supramolecular Interactions: Coordination Complexes – Organic Radical *Cryst. Growth Des*. **2017**, *17*, 4893-4899.

68 O. V. Dolomanov, L. J. Bourhis, R.J . Gildea, J. A. K. Howard, H. J. Puschmann, OLEX2: A Complete Structure Solution, Refinement and Analysis Program. *Appl. Cryst.* **2009**, 42, 339-341.

69 G. M. Sheldrick, SHELXT: Integrating space group determination and structure solution. *Acta Crystallogr.* **2015**, *71*, 3-8.

70 G. M. Sheldrick, A Short History of SHELX. *Acta Crystallogr*. **2007**, *64*, 112-122.

71 I. A. Guzei, An idealized molecular geometry library for refinement of poorly behaved molecular fragments with constraints. *J. Appl. Crystallogr.* **2014**, *47*, 806-809.

72 V. A. Lazarenko, P. V. Dorovatovskii, Y. V. Zubavichus, A. S. Burlov, Y. V. Koshchienko, V. G. Vlasenko, V. N. Khrustalev, High-throughput small-molecule crystallography at the 'Belok' beamline of the Kurchatov synchrotron radiation source: Transition metal complexes with azomethine ligands as a case study. *Crystals*, **2017**, *7*, 11, 325.

73 R. D. Svetogorov, P. V. Dorovatovskii, V. A. Lazarenko, Belok/XSA diffraction beamline for studying crystalline samples at Kurchatov Synchrotron Radiation Source. *Crystal Research and Technology*, **2020**. *55*, 5, 1900184.

74 W. Kabsch, XDS. *Acta Crystallogr*. **2010**, D66, 125-132.

Table 1. Crystallographic data for $3_2Co_8(suc)_4$, $3_2Ni_8(suc)_4$-Ni, $3_2Co_8(suc)_4$-Co and $3_2Zn_6(suc)_2$

	$3_2Co_8(suc)_4$	**$3_2Ni_8(suc)_4$-Ni**	**$3_2Co_8(suc)_4$-Co**	**$3_2Zn_6(suc)_2$**
Compound Formula	$C_{102}H_{118}Co_8N_2O_{44}S_8$	$C_{108}H_{138}N_4Ni_9O_{50}S_8$	$C_{120}H_{162}Co_9N_8O_{54}S_8$	$C_{130}H_{196}N_{14}Zn_6O_{48}S_8$
Crystal class	Triclinic	Tetragonal	Tetragonal	Orthorhombic
λ, Å	0.7927	0.7937	1.54184, CuK_α	0.7931
Space group	*P-1*	$P4_22_12$	$P4_22_12$	*P* bcn
Z	1	2	2	4
Cell parameters	*a* = 12.638(3)Å, *b* = 13.524(3)Å, *c* = 21.208(4)Å, α = 84.09(3)°, β = 84.24(3)°, γ = 64.85(3)°	*a* = 22.981(3)Å, *b* = 22.981(3)Å, *c* = 13.534(3)Å, α = 90 °, β = 90 °, γ = 90 °	*a* = 22.99439(4)Å, *b* = 22.99439(4)Å, *c* = 13.59342(5)Å, α = 90 °, β = 90 °, γ = 90 °	*a* = 31.887(6)Å, *b* = 23.216(5)Å, *c* = 23.261(5)Å, α = 90 °, β = 90 °, γ = 90 °
V, $Å^3$	3257(1)	7148(2)	7187.41(4)	17220(6)
M (g/mol)	2803.90	3077.09	3367.42	3371.70
T, K	100(2)	100(2)	100(1)	100(2)
Size, mm	0.2x0.34x0.43	0.05x0.05x0.10	0.106x0.168x0.32	0.010x0.050x0.050
F(000)	1440	3188	3482	7064
ρ_{calc} g/cm^3	1.429	1.430	1.556	1.301
μ, cm^{-1}	1.623	1.827	9.769	1.340
θ, deg	3.284≤θ≤30.955	1.979≤θ≤31.011	2.718≤ θ ≤ 76.870	1.211≤ θ ≤ 28.141
Refl. meas.	49598	23575	217463	105374
Independ/ Rint	13943/0.0703	8096/0.0498	7477/0.0461	14774/0.1427
Param./restr	694/37	482/107	572/200	964/141
Refl. [I>2σ(*I*)]	10952	6404	7338	9717
R_1 / wR_2	0.1101/0.2865	0.0645/0.1705	0.0484/0.1408	0.0711/0.1866
R_1/wR_2 (all refl.)	0.1267/0.3052	0.0810/0.1856	0.0491/ 0.1417	0.1087/0.2164
Goodness-of-fit	1.022	1.051	1.059	1.025
ρ_{max}/ρ_{min} ($eÅ^{-3}$)	3.147/ -1.608	1.019/ -2.282	2.214/ -1.268	0.791/-0.741
Flack parameter	-	0.031(8)	-0.020(2)	-

Table 2. Observed selected bond distances determined by X -ray diffraction on single crystals.

	$3_2Co_8(suc)_4$	**$3_2Co_8(suc)_4$-Co**	**$3_2Ni_8(suc)_4$-Ni**	**$3_2Zn_6(suc)_2$**
M-O in nanocontainer	2.009(5) 2.017(5) 2.019(5) 2.025(5) 2.030(5) 2.037(4) 2.040(4) 2.050(5) 2.063(4) 2.067(4) 2.074(5) 2.093(5) 2.098(4) 2.100(5) 2.101(5) 2.121(5) 2.145(5) 2.162(4) 2.208(5) 2.217(4) 2.224(4) 2.296(5)	2.015(4) 2.026(4) 2.033(4) 2.045(4) 2.054(3) 2.060(4) 2.094(4) 2.101(4) 2.103(4) 2.119(3) 2.2040(17) 2.2722(17)	1.998(6) 1.999(6) 2.010(6) 2.020(6) 2.032(6) 2.036(5) 2.068(5) 2.072(6) 2.073(5) 2.075(5) 2.168(2) 2.209(2)	2.010(5) (DMF) 2.014(4) 2.018(4) 2.023(4) 2.027(5) 2.028(4) (DMF) 2.047(4) 2.053(4) 2.085(4) 2.090(4) 2.106(4) 2.124(4) 2.129(4) 2.168(4) 2.178(4) 2.211(4)
M-O in $M^{II}(DMF)_4(OH)_2$	-	2.011(6) 2.091(6) 2.114(18) (disorder)	1.958(11) 2.081(8)	-
M-M	2.9924(16) 3.0071(15) 3.0104(15) 3.0186(16)	3.0059(11) 3.0218(11)	2.9673(15) 2.9791(14)	3.0122(10) 3.0267(10)

Table of Content

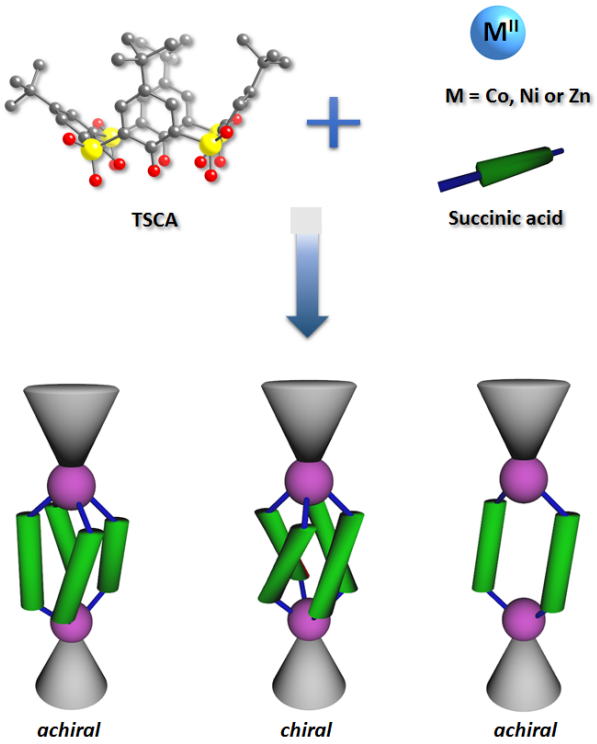

The formation of three types of Supramolecular Coordination Cages is described, using the-three-components approach. The use of tetrasulfonylcalixarene, combined with metallic salts (Ni, Co and Zn) and the flexible succinate ancillary ligand, led to cages displaying different size of cavity. H bonded induced chirality was observed for both isomorphous cages.